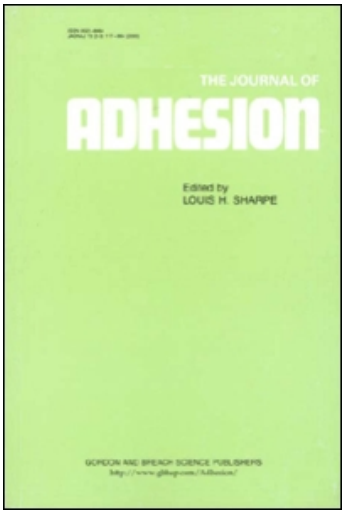

The Journal of Adhesion
Publication details, including instructions for authors and subscription information:
http://www.informaworld.com/smpp/title~content=t713453635

Chemical Aging in Epoxies: A Local Study of the Interphases to Air and to Metals

A. Meiser[a]; K. Willstrand[a]; P. Fehling[a]; W. Possart[a]
[a] Saarland University, Chair for Adhesion & Interphases in Polymers, Saarbruecken, Germany

To cite this Article Meiser, A. , Willstrand, K. , Fehling, P. and Possart, W.(2008) 'Chemical Aging in Epoxies: A Local Study of the Interphases to Air and to Metals', The Journal of Adhesion, 84: 4, 299 — 321
To link to this Article: DOI: 10.1080/00218460802004360
URL: http://dx.doi.org/10.1080/00218460802004360

The Journal of Adhesion, 84:299–321, 2008

ISSN: 0021-8464 print/1545-5823 online
DOI: 10.1080/00218460802004360

Taylor & Francis
Taylor & Francis Group

Chemical Aging in Epoxies: A Local Study of the Interphases to Air and to Metals

A. Meiser, K. Willstrand, P. Fehling, and W. Possart
Saarland University, Chair for Adhesion & Interphases in Polymers, Saarbruecken, Germany

The aging behavior of an epoxy adhesive (DGEBA and DETA) in the bulk surface region and in the contact region to metal substrates (Au, Cu) is studied locally. Therefore, the chemical depth profile during aging is recorded with FTIR microscopy on sample surfaces prepared with low angle microtomy. Two environmental conditions are applied at 60°C for up to 500 days to separate the role of temperature and humidity in aging.

Quantitative evaluation of the IR spectra provides the following results: in the bulk surface region, three aging mechanisms form a gradient region of more than 200 μm. Their intensity and depth profile depend on the environmental conditions. Epoxy-metal contacts are unaffected under dry conditions. Humidity is needed to form a 50 μm thick region where the copper substrate accelerates aging. Based on the experimental results, chemical aging mechanisms are discussed.

Keywords: Aging; Epoxy; FTIR microscopy; Interphase

INTRODUCTION

The aging of adhesives and paints determines the durability of structural bonds and coatings provided corrosion is prevented. In principle, it is well known that the chemical aging of polymers depends on environmental factors such as humidity [1–3], temperature [4–6], irradiation [5,7], gases [8,9], etc. and on the polymer state itself [1,4–6]. In addition, the properties of a polymer adhesive and, therefore, the aging behavior will be influenced by the substrate that

Received 12 October 2007; in final form 5 February 2008.
One of a Collection of papers honoring John F. Watts, the recipient in February 2008 of *The Adhesion Society Award for Excellence in Adhesion Science, Sponsored by 3M*.
Address correspondence to Wulff Possart, The Saarland University, Gebaeude C6.3, P.O. Box 151150, D-66041 Saarbruecken, Germany. E-mail: w.possart@mx.uni-saarland.de

causes the formation of an interphase [10–15]. Despite the great number of publications, the complex interplay of that many factors and parameters is not fully revealed. For a better understanding of aging of adhesives and paints, it is crucial to reveal the chemical processes in the bulk polymer, at its surface, and in the polymer-substrate interphase as a function of the given environmental conditions.

Therefore, the depth profile of the chemical properties has to be studied as a function of time. However, several limitations complicate that experimental task. First, the adhesive bulk and the adherends bury the interphase. This problem can be, in part, circumvented by studying thin films on metal substrates or on fibers with surface sensitive techniques like XPS, TOF-SIMS, UV/VIS, Raman, or FTIR spectroscopy [16–21]. However, the thin film could form a surphase at the contact with the atmosphere. Then, it might be a problem to transfer thin film results to thicker films or to adhesive joints because this surphase could influence the thin film performance. Secondly, depth profiles in real joints are not accessible in a non-destructive way with the aforementioned surface sensitive techniques. Therefore, different sample preparation techniques are proposed in the literature. Focused ion beam milling is promising, but still suffers from ion implantation and from the delicate degradation behavior of polymers [22]. Chemical depth profiling by scratching the sample surface with an abrasive paper (Si-Carb sampling) is reported [23,24]. The spectra of the particles adhering to the paper are measured with diffuse reflectance (DRIFT) but the mechanical abrasion of the polymer might introduce unwanted chemical modification. Repeated microtome sectioning in combination with transmission spectroscopy and microscopy is reported as a method to monitor the depth profile during aging [23–25]. Alternatively, Watts and coworkers described a microtome preparation technique for polymer interphases. Here the sample is cut at a defined ultra low angle with respect to the interphase. Then, the cut surface is studied successfully with XPS and TOF-SIMS [20,21,26].

In this article, a similar preparation technique is utilized and the depth profile in metal-polymer joints is recorded by FTIR microscopy. For the exposed surface zone and for the interphase to gold and copper substrates, the depth profiles are revealed after chemical aging in an epoxy network under dry and wet conditions.

EXPERIMENTAL

Materials and Sample Preparation

The examined epoxy adhesive system consists of the widely used diglycidyl ether of bisphenol A (DGEBA, DOW Chemicals D.E.R. 332

provided by DOW Deutschland GmbH & Co. OHG, Stade, Germany) and the aliphatic curing agent diethylene triamine (DETA, provided by Fluka, Buchs, Switzerland). Curing proceeds at room temperature (RT) by the oxirane ring addition to primary and secondary amine groups, resulting in hydroxyl groups. The chosen mass ratio DGEBA : DETA = 100 : 14 corresponds to a slight excess of amine hydrogen compared with epoxy rings. The monomers are mixed in a closed glass vessel at 55°C for 5 min.

The samples are prepared subsequently in a glove box filled with CO_2-reduced, dried air (dew point: −70°C) to minimize the contact with ambient air in order to avoid parasitic reactions between amine, H_2O, and CO_2.

The liquid epoxy adhesive is cast in a silicone mould with rectangular openings ($1.5 \times 8 \times 12$ mm depth) to produce rectangular epoxy blocks that fit in the sample holder of the microtome. Bulk samples are obtained by covering both sides of the filled mould with PTFE films (25 μm thick) fixed on float glass. Thereby, the epoxy block has smooth and flat surfaces at the top ends ensuring the dimensional accuracy necessary for defined low angle cuts. The chemical conversion of epoxy rings is constant across these bulk samples. Hence, the PTFE film does not influence the cross linking reactions. For the preparation of metal-epoxy interfaces, one of the PTFE films on the filled mould is replaced by a pure copper or gold film (*ca.* 100 nm thick) that was prepared on a silicon wafer by physical vapor deposition.

The samples were cured in dried air at RT for 72 h. The resulting samples show incomplete conversion of epoxy groups. In addition, a post-curing step may follow in argon at 120°C for 1 h. It leads to a completely cured network in bulk. Finally, the samples demold easily due to the poor adhesion on silicone and on PTFE. In the case of metal-epoxy contacts, the wafer is removed after curing by thermal shock leaving the intact metal layer on the epoxy.

Aging Conditions

In the dark and at the moderate aging temperature of 60°C, the samples are exposed to two different environments to discriminate the role of humidity and O_2 in aging: thermo-oxidative aging in dry air (dew point: −70°C), and hygro-thermo-oxidative aging in wet air (90% RH). The depth profile of the chemical modifications during aging is monitored by regular sample characterization during up to 500 d using FTIR microscopy. The μ-ATR spectra are recorded along a line on the surface produced by low angle cutting as described below.

Microtomy

The top face (1.5×8 mm) of each sample is cut on an Ultra Cut E microtome (Reichert, Nussloch, Germany) with diamond knives (Diatome, Biel, Switzerland). Its long side corresponds to the cutting direction and is inclined horizontally by $\alpha = 2^\circ$ to produce a low angle cut with respect to the top surface. Figure 1 visualizes the cutting steps.

At first, both top edges are trimmed with a glass knife that is vertically inclined by 40° until the residual top surface has a width of 0.5 mm at the broader end. This reduces the cutting width and, therefore, the cutting force in the following stepwise sectioning. Then, the top surface is trimmed at the chosen inclination angle with a diamond trimming blade (Diatome ultratrim) until two-thirds of the top surface is removed. The following sections are made with a diamond knife (Diatome ultra AFM) to produce a smooth and artifact-free surface. The cutting force is reduced further by wetting the cutting edge with distilled water. A part of the top surface remains uncut to allow for a precise determination of the cutting angle afterwards and for the study of the aging of the epoxy bulk surface.

White Light Interferometry

The microtomed samples are examined with a white light interferometer (Zygo New View 200, supplied by LOT GmbH, Darmstadt, Germany). The angle between the top surface and the prepared cut surface is determined along four lines perpendicular to the cut edge. The mean value represents the real cutting angle of the sample.

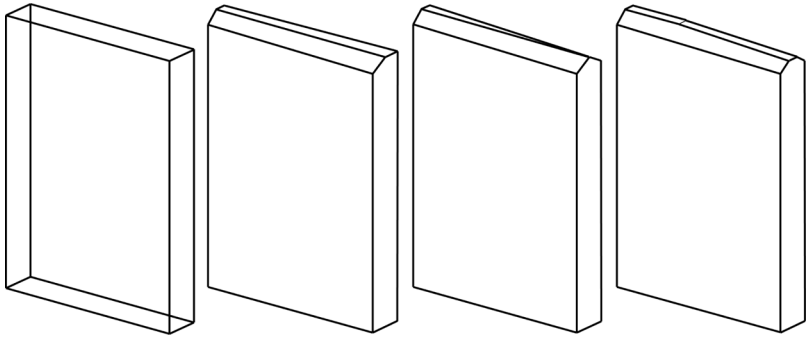

FIGURE 1 Microtomy—principal steps of sample preparation for depth profiling.

FTIR Microscopy

The chemical state of the sample is studied as a function of the distance from the sample surface. For that purpose, a Hyperion 2000 FTIR microscope (Bruker Optik GmbH, Ettlingen, Germany) is used in ATR mode with p-polarized light in the mid IR range (400–4000 cm^{-1}). The germanium crystal of the μ-ATR objective possesses a tip diameter of 100 μm. The lateral distance, l, on the cut surface corresponds to a certain depth, z, below the initial surface or the metal-epoxy interface.

$$z = l \cdot \sin \alpha. \tag{1}$$

Accordingly, a lateral resolution of 100 μm, equal to the tip diameter, corresponds to a depth resolution of 3.5 μm for an inclination angle α of 2°. ATR spectra are recorded point-wise at a minimum distance of 100 μm on the cut surface perpendicularly to the cut edge. Co-addition of 300 scans at each position results in a good signal-to-noise ratio. The sample spectra are divided by an ATR reference spectrum of the atmosphere. This eliminates the optical effects of the ATR crystal, the light source, and the gas atmosphere in the light path. The influence of temporal variations of humidity is minimized by purging the customized sample compartment with dry air. Additionally, the atmospheric compensation function implemented in the software of the spectrometer is applied to eliminate the H_2O and CO_2 bands in each spectrum.

The depth profile of the oxirane consumption and of several aging bands is derived by means of quantitative spectral analysis. The spectroscopic degree of oxirane consumption, U_{EP}^{IR}, is calculated from the peak height, I_{915}, of the band at 915 cm^{-1} normalized to the peak height, I_{1510} of the phenyl ring stretching vibration at 1510 cm^{-1}:

$$U_{EP}^{IR}(z) = 1 - \frac{I_{915}(z)/I_{1510}(z)}{I_{915}^0/I_{1510}^0}. \tag{2}$$

The initial state of the non-reacted epoxy mixture ($t = 0$) cannot be measured as the system starts to react during mixing. It is estimated from the volumetric addition of pure DGEBA and DETA μ-ATR spectra with respect to their masses, m, and densities, ρ, according to Eq. (3).

$$I^0(\tilde{\nu}) = \frac{m_{DGEBA}/\rho_{DGEBA} \cdot I_{DGEBA}(\tilde{\nu}) + m_{DETA}/\rho_{DETA} \cdot I_{DETA}(\tilde{\nu})}{m_{DGEBA}/\rho_{DGEBA} + m_{DETA}/\rho_{DETA}}. \tag{3}$$

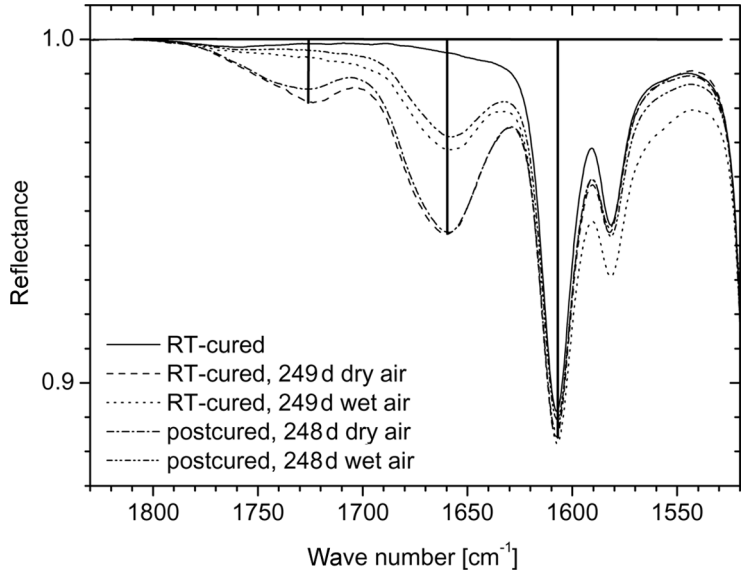

FIGURE 2 Aging bands at 1725, 1660, and 1600 cm^{-1} on the surface of bulk specimens after curing and aging in dry and wet air and the chosen baseline definition.

Furthermore, two new aging bands arise at 1725 and 1660 cm^{-1} and a hidden band increases under the phenylene bands at 1600 cm^{-1} during aging. Their peak heights are determined as shown in Fig. 2 and normalized to the peak height, I_{1510}, according to Eq. (4):

$$\mathrm{I}^{\mathrm{norm}}_{1725}(\mathrm{z}) = \mathrm{I}_{1725}(\mathrm{z})/\mathrm{I}_{1510}(z). \tag{4}$$

For these aging bands at 1725, 1660, and 1600 cm^{-1} a reasonable assignment to chemical groups is proposed in Table 1 (*cf.* [14,27]). Although the assignment is not absolutely free of ambiguity, it

TABLE 1 Assignment for the IR Bands Observed During Aging

IR band (cm^{-1})	1725	1660	1600
Functional group	Ketone, aldehyde, saturated carboxylic acid	Alkene, conjugated alkene (sym.), oxime, imine, enamine, amide	conjugated alkene (asym.), amino salt

provides the starting point for our hypotheses on the chemical aging mechanisms in the epoxy.

RESULTS

Surface Region of Epoxy Bulk Samples: Oxirane Conversion During Aging

Network formation is complete in post-cured bulk samples, whereas, RT-curing results in vitrification at a spectroscopic degree of epoxy conversion of only $\sim$71%. This chemically induced glass transition slows down the epoxy consumption rate by orders of magnitude. Many reactive groups remain in the polymer. They are consumed during aging (Fig. 3). The rate of that ongoing oxirane conversion depends on the aging conditions.

The conversion in dry air proceeds quite homogeneously across the sample. Hence, atmospheric effects are not involved and the curing process simply continues during aging. Oxirane conversion reaches 96% after 50 d of aging (Fig. 3a). Under wet conditions, it takes only 16 d (Fig. 3b) for the same conversion. The penetrated water accelerates the network formation by polymer plasticization [28]. Moreover, water is expected to catalyze the oxirane ring opening reaction [29]. The conversion increases very homogenously in all samples, *i.e.*, the water penetrates the top 200 μm of the epoxy within less than 16 d, thus resulting in a homogenous acceleration of the epoxy conversion in this surphase region to air. This conclusion is supported by the observation that the water uptake of post-cured bulk samples reaches almost equilibrium after only 10 d [28].

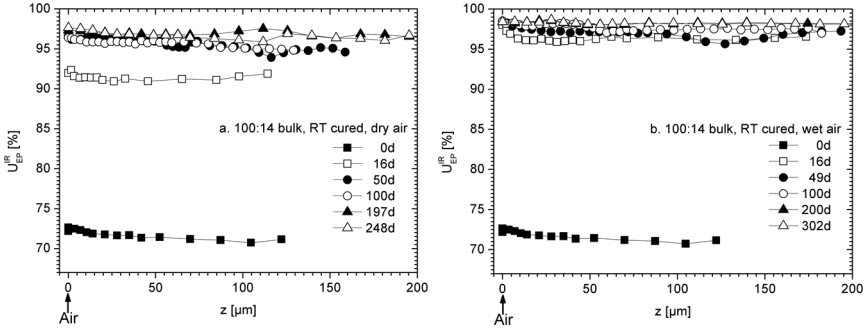

FIGURE 3 Oxirane conversion as a function of position in RT-cured bulk samples during aging in dry and wet air.

Surface Region of Epoxy Bulk Samples: Chemical Aging Effects in Dry Air

A first aging peak at 1660 cm^{-1} rises on the epoxy after 16 d on RT-cured samples and after 50 d on post-cured samples (Figs. 4a,b). The air must cause the corresponding chemical modification as the peak starts close to the epoxy surface before it appears inside the sample. For RT- and post-cured bulk samples as well, the peak height, I_{1660}, increases with time and advances into the material. After 100 d, a 120 μm wide gradient has formed. That inhomogeneous region of chemical modification extends over more than 200 μm after 248 d. Both network states show a quite identical development with respect to I_{1660} (t_{age}, z) until 248 d. In conclusion, the different content of residual reactive groups in the RT- and post-cured samples, especially amine hydrogen, is not the reason for this aging mechanism.

A second aging peak at 1725 cm^{-1} appears after 16 d at the surface of RT-cured samples and after 50 d on the post-cured specimens (Figs. 5a,b). The intensity I_{1725} (t_{age}) also rises and proceeds into the epoxy, but more slowly than I_{1660} (t_{age}). As the result, the gradient of this chemical modification is steeper and reaches only 170 μm into the polymer after 248 d. However, I_{1725} (t_{age}, z) develops simultaneously for the two network states again. Thus, the residual amine hydrogen content does not influence the kinetics of this mechanism either.

Note that the bands at 1660 and 1725 cm^{-1} (Figs. 4 and 5, respectively) do not develop synchronously. In fact, the band at 1660 cm^{-1} extends more quickly over a broader range with a smoother gradient into the epoxy than the band at 1725 cm^{-1} which is restricted to a narrow surface region for the first 100 d. Additionally, they always

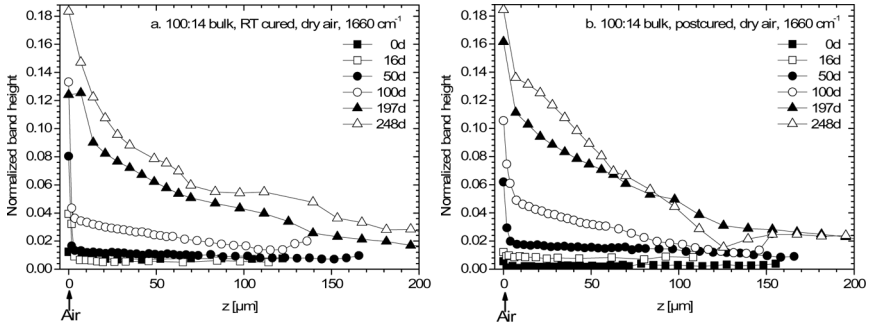

FIGURE 4 Intensity of the aging band at 1660 cm^{-1} in RT- and post-cured bulk samples during aging in dry air.

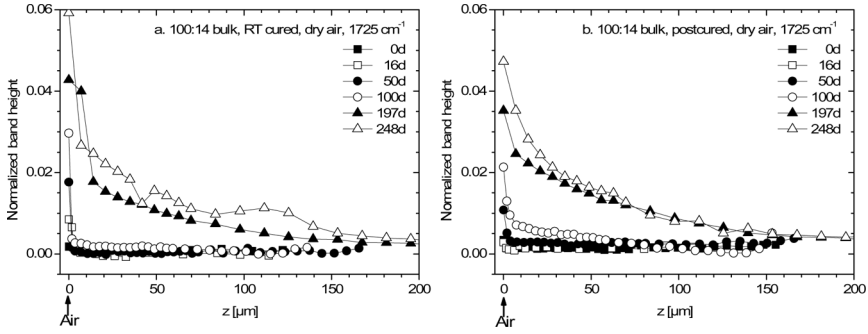

FIGURE 5 Intensity of the aging band at 1725 cm^{-1} in RT- and post-cured bulk samples during aging in dry air.

reach different intensities with I_{1660} (t_{age}, z) $\gg$ I_{1725} (t_{age}, z). According to any IR spectroscopic experience, however, stretching vibrations ν(C=O) absorb strongly, if not very strong, while the IR absorptions of ν(−C=C−) and ν(−C=N−) are weak or at best of medium strength [27]. Therefore, the observed intensity ratio points at a higher concentration of −C=C− and −C=N− species than of C=O species. All these findings indicate that both bands cannot result from only one reaction.

A third spectral change is observed for the band at 1600 cm^{-1} (Fig. 6.) It changes intensity in a more complicated manner. The general level of intensity rises within the first 16 d of aging but then the I_{1600} goes down inside the epoxy. Simultaneously, the peak height increases at the surface after 16 d for RT-cured samples and after 50 d

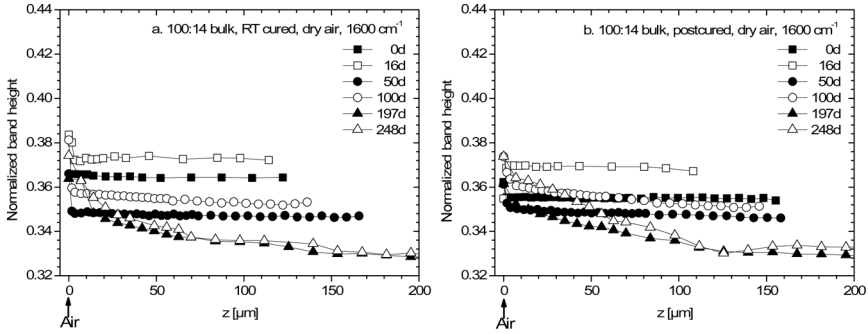

FIGURE 6 Intensity of the aging band at 1600 cm^{-1} in RT- and post-cured bulk samples during aging in dry air.

for post-cured samples. It takes 248 d to extend a gradient of more than 200 μm into both kinds of samples. The development of the gradient in time and space coincides well with the behavior of the aging peak at 1660 cm^{-1}. Once more, RT-cured samples and post-cured samples show a comparable behavior.

Surface Region of Epoxy Bulk Samples: Chemical Aging Effects in Wet Air

In wet air, the band at 1660 cm^{-1} can be found after 16 d at the surface of the RT- and post-cured samples and increases over time (Figs. 7a,b). Contrary to aging under dry conditions, a second maximum in band height appears *ca.* 20 μm beneath the surface after 200 d. The height of this maximum increases and it shifts into the sample in the course of aging. A steep drop in band height and a smooth gradient over more than 200 μm follows the maximum on the bulk side. Thus, a further process like degradation or evaporation leads to this depletion zone. Compared with aging in dry air (*cf.* Fig. 4), the I_{1660} is slightly weaker in the gradient region despite the plasticizing effect of water. This also indicates that the presence of water supports the degradation of the formed product not only in the surface-near region, but also in the bulk.

The band at 1725 cm^{-1} appears close to the surface after 16 d as well (Figs. 8a,b), but is very small compared with aging in dry air (*cf.* Fig. 5). It only affects the top 50 μm after 400 d. Therefore, the presence of water either hinders the formation of the product or leads to its consumption.

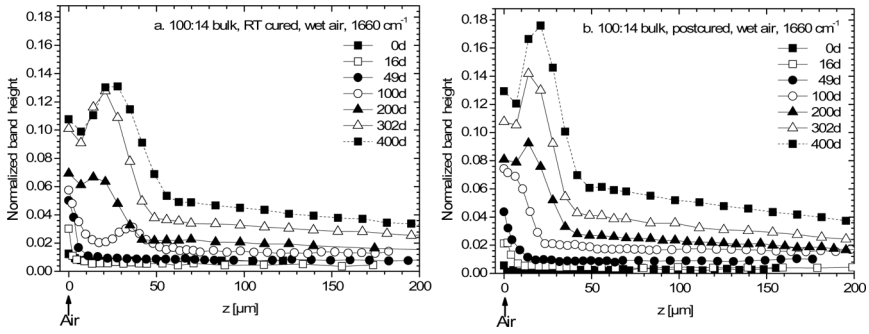

FIGURE 7 Intensities of the aging band at 1660 cm^{-1} in RT- and post-cured bulk samples during aging in wet air.

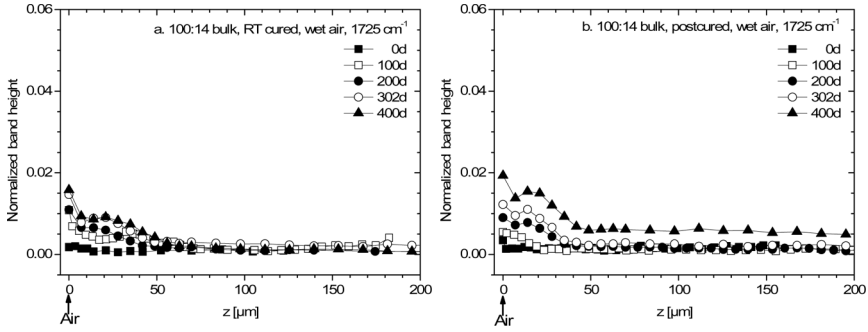

FIGURE 8 Intensities of the aging band at 1725 cm^{-1} in RT- and post-cured bulk samples during aging in wet air.

An increase of the band at 1600 cm^{-1} is observed for RT-cured samples first at the surface after 16 d (Fig. 9). The highest value is reached after 100 d. Afterwards, the intensity drops again indicating a degradation of the formed product. In post-cured samples, I_{1600} increases slowly at the surface over 400 d, but it never reaches the intensity observed on RT-cured samples. Thus, in RT-cured samples the aging mechanism takes advantage of the higher availability of reactants and of the more flexible network in the early stage of aging. In the further course of aging, a second maximum at a depth of 20–40 µm appears in both networks, as for I_{1660}. Therefore, the product behind I_{1600} also degrades under the influence of water as discussed for I_{1660}. Compared with aging in dry air (*cf.* Fig. 6), I_{1600} develops faster and reaches higher values. Thus, the presence of water promotes the mechanism. The bands at 1660 cm^{-1} and

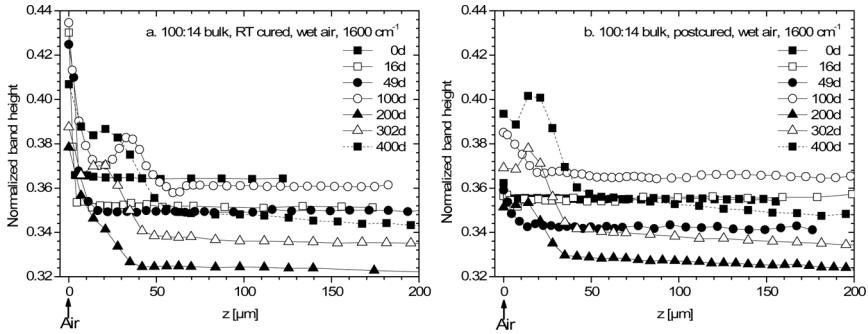

FIGURE 9 Intensities of the aging band at 1600 cm^{-1} in RT- and post-cured bulk samples during aging in wet air.

1600 cm^1 behave similarly and they show higher intensities and a second maximum within the material under wet conditions. Hence, they could arise from the same mechanism.

Metal-Epoxy Contact: Chemical Aging in Dry Air

While the aging of the region near the surface is relevant for coatings, the behavior of the buried interphase in metal substrates is most important for coatings and adhesives as well.

As a first example, the aging of post-cured epoxy-gold samples (full oxirane consumption) is considered under dry aging conditions (Fig. 10). During 500 d, no spectral changes arise on the cut surfaces within the 200 μm zone of the metal-contrary to the bulk surface (see above). Therefore, the thin gold film does not influence the polymer but it acts as an effective protection against the surrounding atmosphere.

As a second example, aging in copper-epoxy specimens is considered. Copper was chosen because it forms complexes with amines during curing [10,30] and because it accelerates degradation in ultra-thin epoxy films [14,31,32].

Post-curing results in full oxirane conversion within the copper-epoxy sample even at a 3 μm distance from the substrate, as in the bulk specimens (not shown). Figure 11 depicts the oxirane conversion within the first 3 μm of the RT-cured epoxy at the Cu contact as a function of aging time under dry and wet conditions. Here, the freshly prepared samples reach the same spectroscopic degree of epoxy conversion as the bulk after RT-curing (~71%). During aging, the samples show a spatially homogeneous oxirane conversion in the

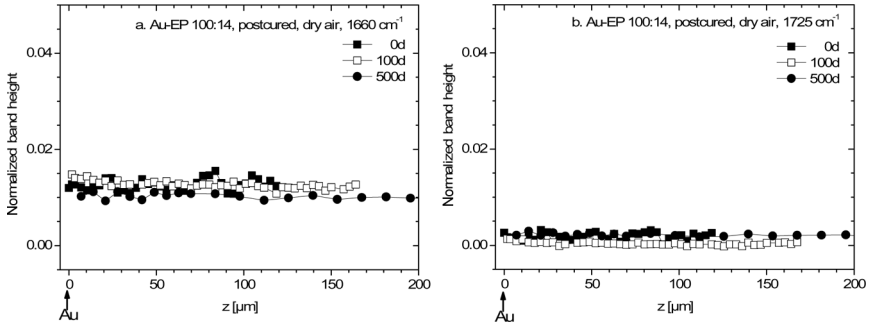

FIGURE 10 Intensities of the aging bands at 1660 and 1725 cm^{-1} in post-cured Au-EP samples during aging in dry air.

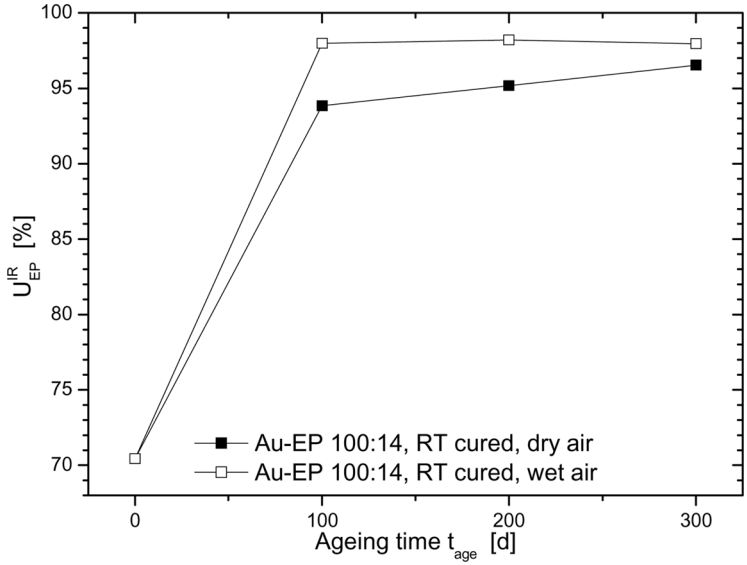

FIGURE 11 Oxirane conversion in RT-cured epoxy in the 3 μm region at the contact with Cu during aging in dry and wet air.

3 μm zone at the metal contact and also deeper in the epoxy (not shown here). Therefore, any influence of the copper substrate on the cross-linking reactions extends less than 3 μm into the freshly formed polymer. The samples reach nearly full epoxy conversion after 300 d in dry air and 100 d in wet air at 60°C. This temporal development and the acceleration by water are in good agreement with the bulk results.

Under dry conditions, no band at 1725 cm^{-1} develops near the substrate during 498 d, both in RT- and post-cured Cu-epoxy samples. Obviously, the aging mechanisms related to I_{1725} need atmospheric oxygen that is available mainly in the surface region of the epoxy. The band at 1660 cm^{-1} increases weakly throughout the whole sample (*cf.* Fig. 12) but it is much weaker than at the epoxy bulk surface. Due to the low I_{1660} no related change of intensity is found for the band at 1600 cm^{-1}.

In conclusion, the aging mechanisms affect mainly the epoxy surface region of some hundred micrometers width under dry conditions. This indicates that the mechanisms need atmospheric oxygen. The oxygen content in the bulk and near the substrate appears to be insufficient to start chemical aging. Cu does not trigger the aging of

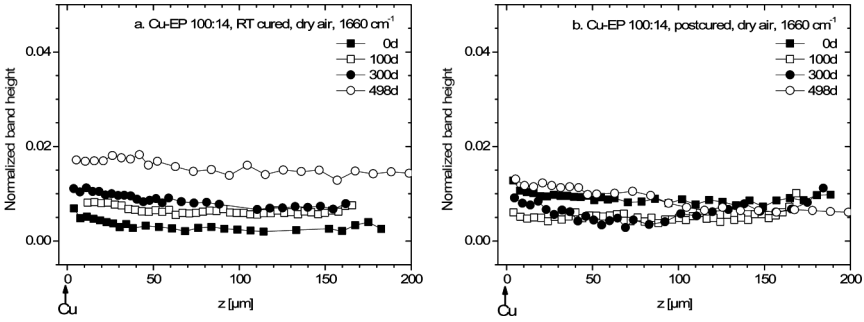

FIGURE 12 Intensity of the aging band at 1660 cm^{-1} in RT- and post-cured Cu-EP samples during aging in dry air.

the epoxy when the interphase is shielded from atmospheric influences by the epoxy bulk.

Metal-Epoxy Contact: Chemical Aging in Wet Air

Contrary to dry aging, the bands at 1660 cm^{-1} and 1600 cm^{-1} develop close to the copper substrate, especially in RT-cured samples (*cf.* Figs. 13,14).

The band at 1660 cm^{-1} forms an intensity gradient that extends over *ca.* 50 µm after 484 d (*cf.* Fig. 13). The gradient is slightly stronger for the RT-cured samples but it is also present in the post-cured specimens. The more flexible network prior to aging, resulting in higher mobility of the reactants, can explain the stronger aging of RT-cured samples. Far from the substrate, I_{1660} develops only slowly

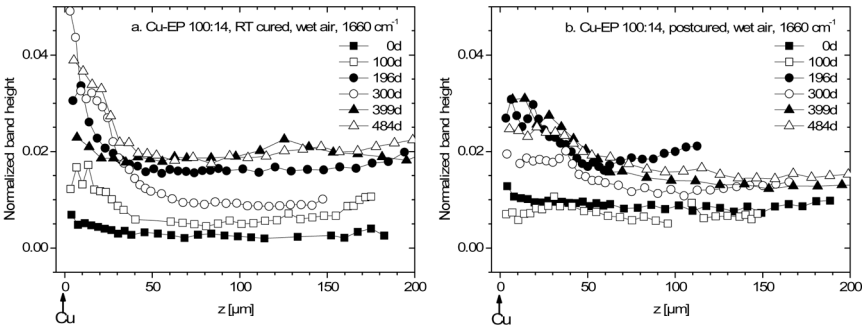

FIGURE 13 Intensity of the aging band at 1660 cm^{-1} in RT- and post-cured Cu-EP samples during aging in wet air.

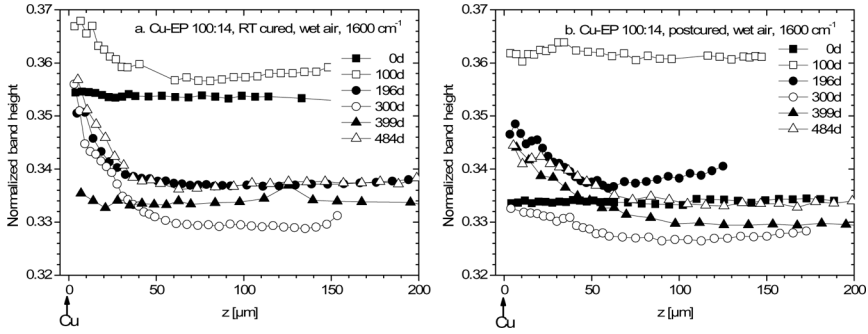

FIGURE 14 Intensity of the aging band at 1600 cm^{-1} in RT- and post-cured Cu-EP samples during aging in wet air.

and weakly. Hence, wet aging conditions force chemical aging in an interphase at copper, too.

The band intensity at 1600 cm^{-1} changes in a more complex manner comparable with the surface (Fig. 14.) The general level of intensity rises within the first 100 d of aging but then I_{1600} goes down inside the epoxy while a gradient of some 50 µm forms at the interphase to copper again. This gradient exists in the same region as the gradient for I_{1660}. Interestingly, no band at 1725 cm^{-1} develops in Cu-epoxy interphase although it is visible at the surface.

In conclusion, the water penetrating through the bulk starts pronounced aging in the Cu-epoxy interphase while the bulk is less affected by the water uptake. Therefore, the copper substrate accelerates the aging in its surroundings under wet conditions. The copper substrate pushes only some of the reactions, however. The absence of the band at 1725 cm^{-1} shows that certain reactions can be suppressed or the others are favored. Thus, the copper substrate leads to a higher selectivity of the aging reactions.

DISCUSSION

For ultra-thin epoxy films on metals, hypotheses on the chemical modification mechanisms under moderate aging conditions have been discussed in previous work [14]. In bulk samples, the interphase in the metal substrate is buried. This increases the diffusion path length for water and gases, hence, decreasing their availability in the interphase. The situation is also different with respect to macromolecular mobility but, in principle, the aging chemistry must be similar in the bulk surface region, at adhesive contacts between metal substrate

and epoxy bulk, and for thin films, provided the metal does not affect the reactions. With these presumptions, possible reactions that result in the chemical groups assigned to the bands emerging in the IR spectra are discussed now.

Surface Region of Epoxy Bulk Samples: Chemical Aging Mechanisms in Dry Air

In post-cured samples, oxirane and primary amine groups are consumed completely while secondary amines are left due to the initial amine excess. Tertiary amine groups forming network nodes and hydroxyl groups resulting from network formation dominate the structure. Therefore, oxirane groups are not involved in aging, but secondary and tertiary amines and hydroxyl groups can be attacked. Additionally, the α-C-atoms to the nitrogen and to the ether bond can be oxidized.

In RT-cured samples, residual oxirane rings, primary and secondary amines are integrated into the chemically vitrified network. Therefore, they can react only by local molecular movements. Nevertheless, oxirane conversion proceeds homogenously throughout the sample. In particular, it proceeds faster than the observed chemical aging processes that start at the surface. Therefore, the oxirane conversion is due to the addition of oxirane and amine groups that reinforce the network; reactions of aging products with oxirane groups are unlikely. The temporal separation of cross-linking and aging diminishes the differences in the availability of functional groups and of the chemical structure between initially RT and post-cured samples for the aging reactions. This explains why both network states show a comparable behavior of all aging bands. Thus, reactions of primary amines are unimportant for the observed aging bands. As a consequence, only secondary and tertiary amines, hydroxyl groups, or backbone C-atoms can be involved in the aging mechanisms in dry air. Secondary amine groups can oxidize to oxime ($1660\,cm^{-1}$) and aldehyde ($1725\,cm^{-1}$) [33]:

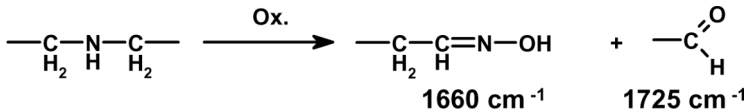

(5)

However, I_{1725} and I_{1660} do not develop synchronously. In consequence, the oxidation of secondary amines can contribute to both observed bands, but it cannot be the only reaction mechanism.

Tertiary amines are also reported to be oxidized by molecular oxygen. The reaction results in backbone scission that weakens the network [6]:

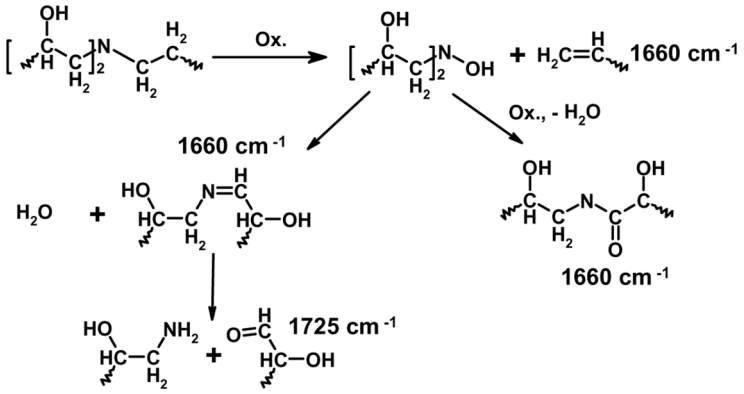

(6)

Via Cope elimination, an alkene (1660 cm^{-1}, as shown) or a hydroxyl alkene (1660 cm^{1}, not shown) is formed depending on the position of the cleavage. The latter can be transformed into the more stable keto form (1725 cm^{-1}). According to the literature, the Cope elimination takes place at more than 100°C. Nevertheless, the breaking of amine cross-links in the network nodes could proceed slowly at the moderate aging temperature. The unstable hydroxylamine, the second product of the Cope elimination, can convert on a first route into an imine (1660 cm^{-1}) that can decompose in the presence of water into a primary amine and an aldehyde (1725 cm^{-1}). As a second reaction path, the formation of amide groups (1660 cm^{-1}) *via* nitrone and oxaziridine intermediates (not shown) is proposed [6]. As all products can explain the observed aging bands, both reaction paths are possible according to our study.

In principle, the OH-groups in the network can oxidize slowly to ketones (1725 cm^{-1}):

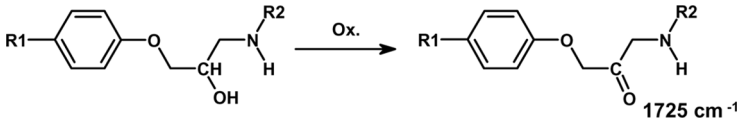

(7)

However, high temperatures and catalysts are needed for quantitative ketone formation [34]. Therefore, this reaction seems unlikely in the epoxy bulk.

Part of the OH-groups in the network could also dehydrate [2]:

(8)

The formed water evaporates. The remaining alkene units possess IR bands at about 1660 cm^{-1} and 1600 cm^{-1} that showed a synchronous gradient formation in the spectra.

According to the literature on aging in the epoxy bulk (*e.g.* [2,4,5,8,9,35,36]), C-atoms in the α-position to tertiary amine groups and to the ether group experience preferential radical oxidation with O_2 to carbonyl (1730 cm^{-1}) and amide (1660 cm^{-1}) groups at 100–250°C or under UV irradiation at moderate temperatures. For our samples, aging is studied at a moderate temperature of 60°C and in the dark, but the studied period is much longer than in the cited literature, and the oxidation by molecular oxygen is also observed at RT [34]. Therefore, radical oxidation might also contribute to the observed band development:

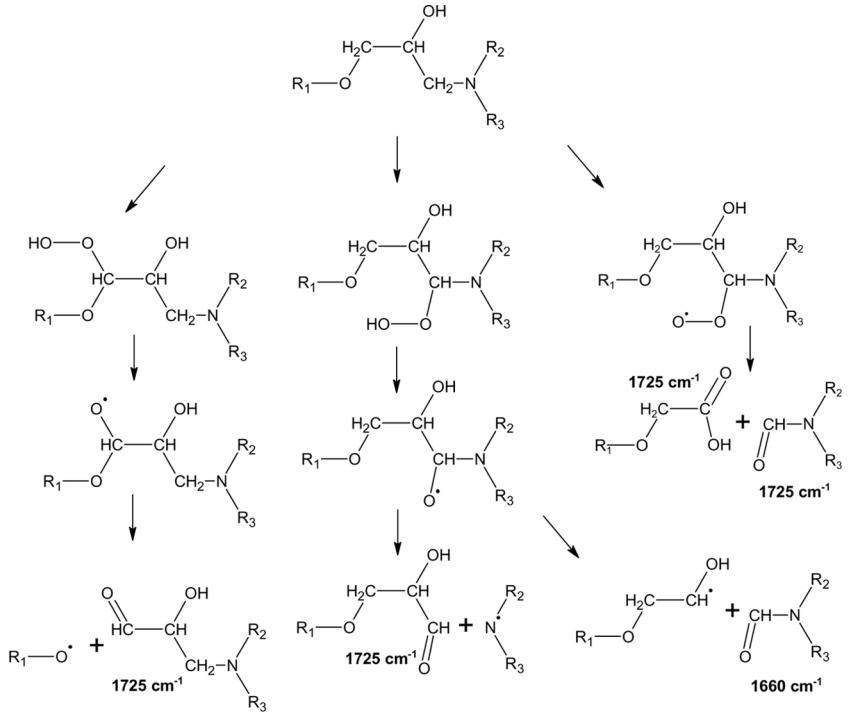

(9)

Alkyl radicals and molecular oxygen form peroxy radicals that transfer their radical state to reactive groups. In the epoxy, the α-C-atoms at tertiary amine groups and at the ether group are attacked preferentially. The resulting hydroperoxides tend to dissociate. The final oxidation products, such as carbonyls (ketones or aldehydes), amides, or carboxylic acids are formed by peroxy decomposition with network cleavage. Such radical oxidation processes can also explain the IR band at 1725 cm^{-1} and at 1660 cm^{-1} observed in bulk aging.

Some of the carbonyls formed according to Eqs. (5)–(7), and (9) could react with residual secondary amine groups to form enamines (1660 cm^{-1}) – *cf.* Eq. (10) for a ketone. This reaction could also contribute to the most pronounced band. However, no decrease of I_{1725} is observed. Therefore, the consumption of carbonyl groups is at least slower than their formation. This is reasonable because both species are integrated into the network. Therefore, their reaction is limited by the low molecular mobility:

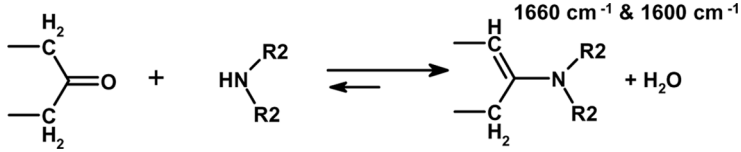

(10)

In conclusion, all the presented aging reactions need oxygen. This explains why the chemical aging starts at the bulk surface and proceeds into the material. As the bands form steep gradients from the epoxy surface into the bulk, the kinetics of all mechanisms is controlled by the diffusion of oxygen. The band at 1725 cm^{-1} indicates the formation of carbonyl or carboxyl groups while the origin of the band at 1660 cm^{-1} can be attributed to oximes, amides, enamines, and alkenes. As conjugated alkenes also absorb at 1600 cm^{-1}, their formation would explain the synchronous development of the band at 1600 cm^{-1}. Nevertheless, several reaction routes are possible to form these products under dry conditions. In particular, it cannot be decided whether the aging is dominated by the oxidation of secondary or tertiary amines or by the oxidation of backbone C-atoms.

Surface Region of Epoxy Bulk Samples: Chemical Aging Mechanisms in Wet Air

In wet air, water plasticizes the stiff epoxy network and leads to a T_g depression from 131 to 99°C in the post-cured bulk [28]. Water also

catalyzes the opening of oxirane rings. Thus, its presence accelerates the oxirane-amine addition. Therefore, the RT-cured samples quickly reach full oxirane conversion as found in the spectra and a network state comparable with post-cured samples leading to the observed synchronous development of chemical aging.

The plasticization of the network enhances any macromolecular mobility and molecular diffusion processes. Therefore, the reactions found under dry aging conditions should be accelerated, but the influence of water on the equilibrium and its reaction with the products must be taken into account. Additionally, water molecules accumulate at polar groups of the network like amines and hamper their oxidation by protonation.

While water only slightly accelerates the formation of the band at 1600 cm^{-1}, the band at 1725 cm^{-1} develops much more weakly in wet air. On the one hand, the formation of the carbonyl species [Eqs. (5)–(7), and (9)] may be hindered in two ways. First, a partial protonation of secondary and tertiary amine groups would hinder their oxidation according to Eqs. (5) and (6). Secondly, the formation of the amide (1660 cm^{-1}) after Cope elimination [Eq. (6)] may be favored under wet conditions compared with the formation of the imine that would produce water and a carbonyl (1725 cm^{-1}). On the other hand, formed carbonyl species might immediately react with water. Therefore, some hydrolytic reactions should be taken into account:

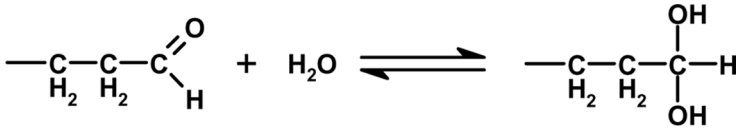

(11)

The comparable intensities of the band at 1660 cm^{-1} under dry and wet conditions leads to the conclusion that the dehydration of hydroxyl groups is unlikely to be the origin of this band. The penetrating water should push the back reaction, especially at the surface where the band actually arises-first. As their oxidation is ruled out above, the hydroxyl groups formed during cross-linking are hardly involved in the observed aging processes.

The formed maximum in peak intensity of the bands at 1660 and 1600 cm^{-1} is due to a maximum of concentration of the corresponding light-absorbing chemical species. Moreover, a concentration maximum indicates *two* or more competing processes of formation and consumption of the chemical species. There are at least two possible explanations for the depletion at the surface. On the one hand, the chemical species belonging to I_{1660} degrades under the influence of water. The product is volatile and diffuses to the sample surface where it

evaporates. This leads to the observed depletion in the near surface region and pushes the degradation into the epoxy specimen. The higher maximum in post-cured samples is due to the fully cross-linked network. Here, the very low polymer mobility hinders diffusion and evaporation of volatiles. However, no such degradation mechanism can be proposed as there are several mechanisms [Eqs. (5), (6), (8)–(10)] and products that might be responsible for the band. On the other hand, the plasticization of the network can explain the depletion without further chemical reaction. By the enhanced molecular mobility, volatile network fragments can more easily diffuse to the surface and evaporate, than under dry conditions, leading to the depletion zone. In fact, such short fragments have been found with electron stimulated ionization mass spectroscopy (ESI-MS) in the immersion bath of epoxy bulk samples [28].

Metal-Epoxy Contact: Chemical Aging Mechanisms

For the epoxy bulk on a copper substrate, the copper surface does not activate any aging reaction under dry conditions. Obviously, the oxygen concentration near the copper surface and in deeper regions of the bulk is insufficient to start chemical aging processes. Therefore, aging is limited to the surface region.

In wet air, the fast water uptake within 10 d does not lead to aging in the bulk. Therefore, the oxygen concentration still is insufficient in the bulk. Nevertheless, a 50 μm broad zone of accelerated aging is detected near the copper substrate. Thus, certain reactions leading to the bands at 1660 and 1600 cm^{-1} are promoted close to the metal when water is present. The absence of the band at 1725 cm^{-1} indicates that the −C=C− or −C=N− species, corresponding to the bands at 1660 and 1600 cm^{-1}, form more easily than the carbonyls and consume all the oxygen available on the substrate.

CONCLUSIONS

The presented preparation method is well suited for studies of the depth profile of aging in polymers, both in the interphases with air and with metals.

The spectra show that the applied aging conditions promote the ongoing curing as long as oxirane groups are available, despite the glassy state of the epoxy. Water accelerates the network formation. As cross-linking proceeds faster than the aging reactions, RT-cured samples quickly reach a network structure comparable with post-cured

samples. Therefore, the temporal and local development of aging is similar in both networks.

In the surface region of epoxy bulk samples, different degradation processes take place under moderate aging conditions and form gradients from the surface to more than 200 μm in depth. Two bands at 1660 and 1600 cm^{-1} develop quite synchronously under dry and wet conditions as well. Humidity does not accelerate the reaction, but leads to a depletion zone at the surface. That points to a degradation or evaporation of the aging products under the influence of water. The band at 1725 cm^{-1} is only observed in a narrow region close to the surface. It is stronger under dry conditions. Thus, at least two independent aging mechanisms are active. They are based on diffusion-controlled oxidation and they attack either secondary or tertiary amines or backbone C-atoms. However, the assignment of the observed bands to chemical reaction remains ambiguous. Further experiments are under way to solve this problem: Samples with other DGEBA: DETA ratios are studied under the same aging conditions to lighten the role of secondary amines in aging. Additionally, a higher aging temperature is chosen to check if aging under more severe conditions follows the same reaction routes as under moderate conditions.

Copper-metal interphases show no aging under dry conditions, but wet conditions activate aging in a surprisingly large zone of 50 μm depth. Similar studies are under way for other metals in order to check their influence on aging from a more general point of view. Further studies will show how far the chemical modifications observed in interphases during aging will affect the mechanical performance of the adhesive joint.

REFERENCES

[1] Carfagna, C., Mastronardi, P., and Nicolais, L., *J. Mater. Sci.* **17**, 2239–2244 (1982).
[2] Luoma, G. A. and Rowland, R. D., *J. Appl. Polym. Sci.* **32**, 5777–5790 (1986).
[3] De Neve, B. and Shanahan, M. E. R., *The Journal of Adhesion* **49**, 165–176 (1995).
[4] Barral, L., Cano, J., López, J., López-Bueno, I., Nogueira, P., Abad, M. J., and Ramírez, C., *Eur. Polym. J.* **36**, 1231–1240 (2000).
[5] Bellenger, V. and Verdu, J., *J. Appl. Polym. Sci.* **30**, 363–374 (1985).
[6] Burton, L. B., *J. Appl. Polym. Sci.* **47**, 1821–1837 (1993).
[7] Zhang, G., Pitt, W. G., Goates, S. R., and Owen, N. L., *J. Appl. Polym. Sci.* **54**, 419–427 (1994).
[8] Buch, X. and Shanahan, M. E. R., *Polym. Degrad. Stab.* **68**, 103–411 (2000).
[9] Buch, X. and Shanahan, M. E. R., *J. Appl. Polym. Sci.* **76**, 987–992 (2000).
[10] Aufray, M. and Roche, A. A., Properties of the interphase epoxy-amine/metal: Influences from the nature of the amine and the metal, in *Adhesion-Current Research and Application*, W. Possart (Ed.) (Wiley-VCH, Weinheim, 2005), pp. 89–102.

[11] Bentadjine, S., Roche, A. A., and Bouchet, J., Epoxy-diamine adhesives on metals: The interphase formation and characterization, in *Adhesion Aspects of Thin Films*, K. L. Mittal (Ed.) (VSP, Utrecht, 2001), pp. 239–260.
[12] Fata, D., Bockenheimer, C., and Possart, W., Epoxies on stainless steel-curing and aging, in *Adhesion-Current Research and Application*, W. Possart (Ed.) (Wiley-VCH, Weinheim, 2005), pp. 479–506.
[13] Fata, D. and Possart, W., *J. Appl. Polym. Sci.* **99**, 2726–2736 (2006).
[14] Meiser, A., Wehlack, C., and Possart, W., Chemical processes during aging in ultra-thin epoxy films on metals, in *Adhesion-Current Research and Application*, W. Possart (Ed.) (Wiley-VCH, Weinheim, 2005), pp. 445–463.
[15] Possart, W., Krüger, J. K., Wehlack, C., Müller, U., Petersen, C., Bactavachalou, R., and Meiser, A., *C. R. Acad. Sci., Ser. IIc: Chim.* **9**, 60–79 (2006).
[16] Boerio, F. J., Hong, P. P., Tsai, H. W., and Young, J. T., *Surf. Interface Anal.* **17**, 448–456 (1991).
[17] Gerlock, J. L., Smith, C. A., Cooper, V. A., Dusbiber, T. G., and Weber, W. H., *Polym. Degrad. Stab.* **62**, 225–234 (1998).
[18] Gerlock, J. L., Prater, T. J., Kaberline, S. L., Dupuie, J. L., Blais, E. J., and Rardon, D. E., *Polym. Degrad. Stab.* **65**, 37–45 (1999).
[19] Dieckhoff, S., Brockmann, W., Faupel, F., and Possart, W., *Adhäsions-und Alterungsmechanismen in Polymer-Metall-Übergängen*, Report BMBF-Project No. 03D0074, (Bremen, 2004).
[20] Hinder, S. J., Lowe, C., Maxted, J. T., and Watts, J. F., *Surf. Interface Anal.* **36**, 1575–1581 (2004).
[21] Hinder, S. J., Lowe, C., Maxted, J. T., and Watts, J. F., *J. Mater. Sci.* **40**, 285–293 (2005).
[22] Sivel, V. G. M., van den Brand, J., Wang, W. R., Mohdadi, H., Tichelaar, F. D., Alkemade, P. F. A., and Zandbergen, H. W., *Journal of Microscopy* **214**, 237–245 (2004).
[23] Adamsons, K., *Prog. Org. Coat.* **45**, 69–81 (2002).
[24] Dumont, N. and Depecker, C., *Vib. Spectrosc.* **20**, 5–14 (1999).
[25] Audouin, L., Anton-Prinet, C., Verdu, J., Mur, G., and Gay, M., *Angew. Makromol. Chem.* **261–262**, 25–34 (1998).
[26] Watts, J. F., The interfacial chemistry of adhesion: Novel routes to the Holy Grail? in *Adhesion-Current Research and Application*, W. Possart (Ed.) (Wiley-VCH, Weinheim, 2005), pp. 1–16.
[27] Socrates, G., *Infrared Characteristic Group Frequencies*, (John Wiley & Sons, Chichester, 1994), 2nd ed.
[28] Bockenheimer, C., Fata, D., and Possart, W., *J. Appl. Polym. Sci.* **91**, 369–377 (2004).
[29] Smith, I. T., *Polymer* **2**, 95–108 (1961).
[30] Bentadjine, S., Petiaud, R., Roche, A. A., and Massardier, V., *Polymer* **42**, 6271–6282 (2001).
[31] Hong, S. G. and Wang, T. C., *J. Appl. Polym. Sci.* **52**, 1339–1351 (1994).
[32] Hong, S. G., *Polym. Degrad. Stab.* **48**, 211–218 (1995).
[33] Metzger, H., Oxime, in *Methoden Der Organischen Chemie* (Houben-Weyl), Band XI/1: Stickstoffverbindungen II, E. Müller (Ed.) (Georg Thieme Verlag, Stuttgart, 1957).
[34] Becker, H. G. O., *Organikum*, (VEB Verlag der Wissenschaften, Berlin, 1988), p. 17, durchgesehene Auflage.
[35] Colin, X., Marais, C., and Verdu, J., *Polym. Test.* **20**, 795–803 (2001).
[36] Damian, C., Espuche, E., and Escoubes, M., *Polym. Degrad. Stab.* **72**, 447–458 (2001).